U.S. National Library of Medicine
National Center for Biotechnology Information

**NLM Citation:** Zhang H. 4,5-Diethyl-10,23-dimethyl-9,24-bis(3-hydroxypropyl)-16,-17-bis(3,hydroxypropyl)oxy-13,20,25,26,27—pentaazapentacyclo-[20.2.1.1$^{3,6}$.1$^{9,11}$.0$^{14,19}$]heptacosa-3,5,8,10,12,14,16,18,20,22,24-undecaene gadolinium hydrates. 2007 Dec 6 [Updated 2008 Jan 8]. In: Molecular Imaging and Contrast Agent Database (MICAD) [Internet]. Bethesda (MD): National Center for Biotechnology Information (US); 2004-2013.
**Bookshelf URL:** https://www.ncbi.nlm.nih.gov/books/

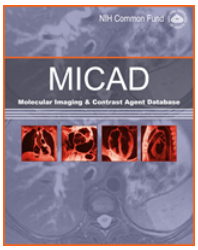


# 4,5-Diethyl-10,23-dimethyl-9,24-bis(3-hydroxypropyl)-16,-bis(3,hydroxypropyl)oxy-13,20,25,26,27—pentaazapentacyclo-[20.2.1.1$^{3,6}$.1$^{9,11}$.0$^{14,19}$]heptacosa-3,5,8,10,12,14,16,18,20,22,24-undecaene gadolinium hydrates

MGd

Huiming Zhang, PhD[1]

Created: December 6, 2007; Updated: January 8, 2008.

| | |
|---|---|
| **Chemical name:** | 4,5-Diethyl-10,23-dimethyl-9,24-bis(3-hydroxypropyl)-16,-17-bis(3,hydroxypropyl)oxy-13,20,25,26,27—pentaazapentacyclo-[20.2.1.1$^{3,6}$.1$^{9,11}$.0$^{14,19}$]heptacosa-3,5,8,10,12,14,16,18,20,22,24-undecaene gadolinium hydrates |
| **Abbreviated name:** | MGd |
| **Synonym:** | Motexafin gadolinium, Gadolinium texaphyrin, Xcytrin, Gd-Tex, PCI-0120, Gd texaphyrin, GdT2B2 |
| **Agent category:** | Small molecule |
| **Target:** | Other |
| **Target category:** | Other |
| **Method of detection:** | Magnetic Resonance Imaging (MRI) |
| **Source of signal/ contrast:** | Gadolinium |
| **Activation:** | No |
| **Studies:** | • *In vitro*<br>• Rodents<br>• Non-primate non-rodent mammals<br>• Humans |

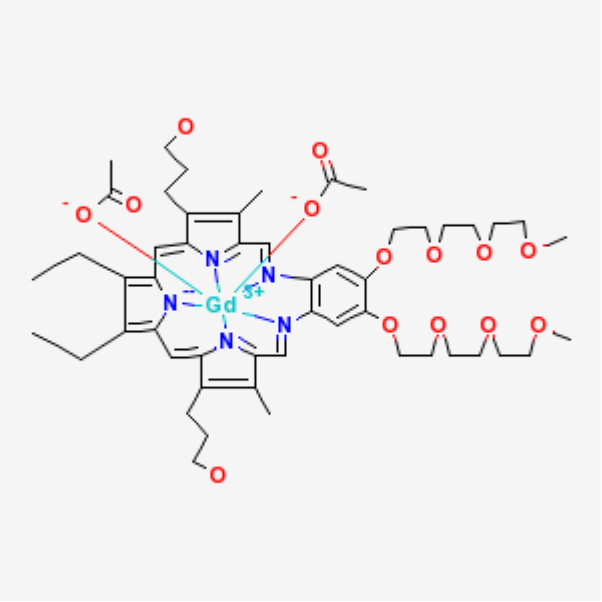


Click on the above structure for additional information in PubChem.

**Author Affiliation:** 1 National Center for Biotechnology Information, NLM, NIH, Bethesda, MD; Email: micad@ncbi.nlm.nih.gov.

# Background

[PubMed]

Porphyrins are well known to be selectively localized in tumors, although the mechanism is not completely understood (1). Certain metalloporphyrins have demonstrated a high affinity for a variety of tumor types including carcinoma, sarcoma, neuroblastoma, and melanoma (2, 3). Combined with the ability to enhance relaxation rates of water protons, metalloporphyrins containing paramagnetic metals like Mn(II) exhibit significant efficacy for the detection, delineation, and staging of tumors in magnetic resonance imaging (MRI) (2, 4). Compared with the use of labeled antibodies for tumor-specific imaging, this approach is not limited by antibody specificity and has high tumor uptake and low cost per dose (2). Gadolinium (Gd) as a lanthanide cation can provide higher efficacy to enhance contrast than manganese because it has seven unpaired electrons instead of five (5). However, porphyrin-related tetrapyrrole macrocycles are inadequate to accommodate large cations like lanthanides (6). Thus, an unprecedented porphyrin-like aromatic ligand named texaphyrin has been synthesized by expanding the macrocycle of porphyrins (7). This novel macrocycle has a pentadentate binding core in a near-circular structure with ~20% larger capacity compared to the tetrapyrrolic analogs of porphyrins (7, 8).

Texaphyrin Gd is a highly stable complex widely known as motexafin Gd (abbreviated as MGd) (9). The Gd(III) cation in the complex is coordinated to all five core nitrogen atoms in a 1:1 fashion and leaves four coordinated sites for the structural water molecules in the inner shell (7). The $T_1$ relaxivity is approximately three to four times greater than that of conventional contrast agents such as gadolinium-diethylenetriamine pentaacetic acid (Gd-DTPA) (10). The open architecture and large number of side chains also provide ample opportunity to outer sphere interactions by hydrogen bonding to the ligand or by close translation of water molecules (10). Unlike many metalloporphyrins, MGd is not a photosensitizer because the strong paramagnetism of the Gd(III) cation promotes efficient relaxation of the excited electronic state (10, 11). The lipophilicity and hydrophilicity in the ligand texaphyrin can be manipulated to enhance the efficacy of selective tissue targeting (10).

MGd has multiple potential applications in cancer treatments in addition to its use in MRI, such as being a single therapeutic agent, either in conjunction with other anticancer agents or concomitantly with radiation therapy (9). This arises from the fact that the ligand can formulate as an 18 π-electron annulene or as an overall 22 π-electron system (8). Therefore, MGd has a high electron affinity and is easily reduced (half-wave potential -0.041 mV *versus* normal hydrogen electrode) (9, 11). *In vivo*, MGd is a redox mediator that catalyzes slow oxidation of intracellular reducing metabolites such as ascorbates, glutathione, dihydrolipoate, nicotinamide adenine dinucleotide phosphate (NADP), and protein thiols and generates superoxide and reactive oxygen species (ROS) for the repair of oxidative radiation and chemotherapy damage (9). MGd is currently undergoing several clinical trials as a radiation sensitizer for brain metastases in conjunction with whole-brain radiation therapy (WBRT). It is also being actively investigated in clinical trials for the treatment of pediatric brain tumors, non-small cell lung cancers (NSCLC), lymphomas, renal cell carcinomas, and pancreatic and biliary tumors (9).

# Synthesis

[PubMed]

The ligand 4,5-diethyl-10,23-dimethyl-9,24-bis(3-hydroxypropyl)-16,-17-bis(3,hydroxypropyl)oxy-13,20,25,26,27—pentaazapentacyclo-[20.2.1.1$^{3,6}$.1$^{9,11}$.0$^{14,19}$]heptacosa-3,5,8,10,12,14,16,18,20,22,24-undecaene was obtained through multiple steps of synthesis (7). First, 2-(acetoxymethyl)-5-((benzyloxy)carbonyl)-4-methyl-3-((methoxycarbonyl)ethyl)pyrrole was reacted with 3,4-diethylpyrrol to produce 2,5-bis[(5-((benzyloxy)carbonyl)-3-((methoxycarbonyl)ethyl)-4-methylpyrrol-2-yl)methyl]-3,4-diethylpyrrole in 75%

yield. The product was further reduced by $BH_3$ in tetrahydrofuran (THF) to produce 2,5-bis[(5-((benzyloxy)carbonyl)-3-(3-hydroxypropyl)-4-methylpyrrol-2-yl)methyl]-3,4-diethylpyrrole in 85% yield, followed by hydrogenation using 10% Pd/C to produce 2,5-bis[(3-(3-hydroxypropyl)-5-carboxyl-4-methylpyrrol-2-yl)methyl]-3,4-diethylpyrrole in near-quantitative yield. Then, the obtained compound was reacted with triethyl orthoformate and dialdehyde tripyrrane in two successive steps to produce 2,-5-bis[(5-formyl-3(3-hydroxypropyl)-4-methylpyrrol-2-yl)methyl]-3,4-diethylpyrrole in 80% yield. Finally, the product was reacted with 1,2-diamino-4,5-bis((3-hydroxypropyl)oxy)benzene to produce the ligand, which formed a complex with $Gd(NO_3)_3$ to give the chelate in 72% yield. The molecular weight of MGd was found to be 972.

MGd is commercially available (Pharmacyclics Inc, Sunnyvale, CA) and is currently undergoing a variety of clinical trials (9), including several phase III clinical trials for the treatment of brain metastasis of lung cancer in conjunction with WBRT (12-14), a phase I clinical trial for the treatment of newly diagnosed glioblastoma multiforme (15, 16), and a phase II clinical trial in patients with lymphoma and multiple myeloma (16).

## *In Vitro* Studies: Testing in Cells and Tissues

[PubMed]

Nuclear magnetic relaxation dispersion (NMRD) and electron spin resonance spectroscopy at x-band were used to examine the relaxation properties for MGd in saline and in 5% human serum albumin (HSA) solution (17). The kinetic parameters were extracted by fitting the experimental NMRD curves, including the rotation correlation time ($\tau_R$) of 120 ps, the electronic relaxation time ($\tau_v$) of 46 ps, the structural water residual time ($\tau_m$) of ~10 ns, and the water coordination number (q) of 3.5 at 37°C. The proton relaxivity of aqueous MGd displayed much higher values than that of the conventional Gd contrast agents in the range of 0.01–50 MHz. For instance, the $T_1$ relaxivity was 19.0 ± 1.5 $mM^{-1}s^{-1}$ at 20 MHz and 25°C *versus* 16.9 ± 1.5 $mM^{-1}s^{-1}$ at 50 MHz and 37°C. These high relaxivity values may be attributed quite simply to a combination high q and long $\tau_R$. In the presence of HSA, the relaxivity of MGd increased, but it was still less than the value predicted from the $\tau_R$ of 3 ns, which reflected a reduced q and/or longer $\tau_m$. Temperature-dependent measurements indicated that the relaxivity of MGd was limited by water exchange in HSA solution but not in aqueous solution. MGd was very stable and no free $Gd^{3+}$ was detected after 7 days. The possible binding of anions like monohydrogen phosphate and dihydrogen phosphate reduced the number of axial coordination sites available for the inner-sphere water complex, as shown in the sharp decrease of the relaxivity from 18 $mM^{-1}s^{-1}$ in aqueous solution to 5.3 $mM^{-1}s^{-1}$ in 0.01 M $KH_2PO_4/K_2HPO_4$ buffer at 25°C and 50 MHz.

The *in vitro* intranuclear uptake of MGd was conducted in four well-established human glioblastoma multiforme cell lines, including T98G, U87, MO59K, and TB10 (18). A solution of 2.3 mg/ml MGd in 5% aqueous mannitol was added to the culture medium to yield a final Gd concentration of 100 μM. After 72 h incubation, the intracellular Gd was found to be 2.5 to 7.5 times greater than the extracellular Gd using inductively coupled plasma mass spectrometry (ICP-MS), and nearly 90% of intracellular Gd was located inside the nuclei.

## Animal Studies

### Rodents

[PubMed]

Young et al. conducted a pharmacokinetic study in rats at a dose of 4 mg/kg (10). A series of blood samples were taken after a bolus injection of $^{153}Gd$-labeled MGd, and the concentration in blood plasma was measured by gamma (γ) counting. The half-life for the initial arterial phase was 4.2 min and 5.4 min for male and female rats, respectively. The half-life for the steady-state phase was 41.4 min and 35.4 min for male and female rats, respectively. The volume of distribution was calculated to be 0.315 L/kg for male rats and 0.265 L/kg for female

rats. The 50% lethal dose ($LD_{50}$) for rats was found to be 147 mg/kg in males and 116 mg/kg in females. The $LD_{50}$ for mice was 118 mg/kg in males and 102 mg/kg in females.

The biodistribution was measured in healthy rats after a bolus injection of $^{153}$Gd-labeled MGd at a dose of 4 mg/kg ($4 \times 10^6$ counts/min per mg) (10). After 48 h, no detectable counts were found in the urine of male or female animals. The cumulative urine excretion after 96 h was 13.67% of the injected dose (ID) for the males and 10.53% of ID for the females. At 7 days after injection, the cumulative fecal excretion was 64% ID for the males and 77% ID for the females. Apparently, most of the fecal excretion occurred within the first 48 h with continual excretion of 1–2% per day for the remainder of the 7-day study. The liver retained the highest amount of radioactivity, and the retention decreased between 24 hours and 7 days. The decrease in radioactive counts in the liver roughly correlated with the recovery in the feces. After ~1 week, 7% ID and 3% ID remained in the carcasses of males and females, respectively. The liver-to-kidney excretion ratio was approximately 5:1, suggesting that MGd secreted into the biliary system predominantly *via* the liver and subsequently excreted into gastrointestinal tract. There was no retention in brain, heart, stomach, duodenum, tests, ovary, muscle, or fat. The organ biodistribution was consistent with uptake of the drug by the liver and secretion into the bile.

The subchronic toxicity study was performed in healthy rats (10). MGd was intravenously injected on Monday, Wednesday, and Friday of each week for 3 weeks at five doses of 0.0, 2.0, 5.0, 10.0, and 20.0 μmol. No difference was observed in body weight gain, clinical chemistries, and complete blood counts. No gross pathological lesions were seen in any organs or histopathological examinations. The administration of 180 μmol/kg during a 3-week period produced no biochemical or histological abnormality.

$T_1$-Weighted images were acquired for healthy rats on a 1.5-T imager after injection of 17 μmol/kg MGd (10). The percent contrast enhancement increased significantly in the liver and kidney from 5 min to 2 h, and the maximum percent contrast enhancement was 81.7% and 114.9% in the liver and kidney, respectively. At a dose of ≥17 μmol/kg MGd, a slight greenish discoloration appeared on the nose tips, ear tips, and tail; this discoloration vanished in 15 min. The tumor signal enhancement was tested in rats with implanted fibrosarcomas 2.5–3.5 cm in diameter. $T_1$-Weighted images were acquired before and 15 min after a bolus injection of 17 μmol/kg MGd. A 49.7% enhancement was found in the fibrosarcoma 15 min after injection, which was still detectable 28 h later. The change after a bolus injection of MGd was subsequently followed up by MRI at 0 min, 10 min, 1 h, 24 h, and 1 week. These MRI scans detected contrast enhancement of 25%, 23.3%, 23.7%, 11.2%, and 2.55%, respectively, for the 5-μmol/kg dose, and 13.15%, 11.65% 10.4%, 7.05%, and 2.6%, respectively, for the 2.5-μmol/kg dose. Similar results were found in DBA/2N mice with SMT-F neoplasmas or EMT-6 tumors (19).

## Other Non-Primate Mammals

[PubMed]

Contrast enhancement efficacy was examined in rabbits with a V2 carcinoma ~2.5 cm in diameter (10, 20). The signal intensity increased dramatically up to 3.5 h after intravenous administration of 5 μmol/kg MGd. The diffusion of the agent through the tumor allowed clear distinction between the malignant tissues and the normal tissues. For rabbits with a V2 carcinoma in the liver, the study was conducted at a dose of 2.5 μmol/kg. Images were collected at 15 min, 1 h, 2 h, and 24 h. The conspicuity of the V2 carcinoma in the liver was significantly increased, and the contrast/noise ratio (C/N) was 5.5 before injection, 10.90 immediately after injection, 10.90 after 15 min, 9.94 in 1 h, and 9.46 in 2 h. The enhancement allowed for the identification of neoplasmas as small as 1 to 2 mm, which were not detectable without MGd.

## Non-Human Primates

[PubMed]

No publication is currently available.

## Human Studies

[PubMed]

A phase I clinical trial was reported by Rosenthal et al. to determine the maximum tolerated dose (MTD), dose-limiting toxicity (DLT), pharmacokinetics, and biolocalization for a single-dose of MGd alone (21, 22). Thirty-eight patients (median age, 58 yrs; range, 35–77 yrs) with incurable lung cancer ($n$ = 26), cervical cancer ($n$ = 3), or other solid tumors ($n$ = 9) received a total of 41 single administrations. The MTD was found to be 22.3 mg/kg with reversible acute tubular necrosis as the marker for the dose-limiting toxicity. The MGd dose was escalated from 0.6 to 29.6 mg/kg, and dose-limiting reversible renal toxicity was observed at the dose of 29.6 mg/kg. The median half-life of MGd after a single-dose administration was 7.4 h, and the maximum recommended dose for the single administration was 16.7 mg/kg. The frequently reported adverse event was transient green discoloration of skin, mucosa, feces, and urine in all of the patients that received doses ≥7.1 mg/kg. The transient increases in transaminases of grade 1 or grade 2 were observed in <5 patients. The peak appeared 48 h after injection and resolved in 7 days. MRI images demonstrated that some but not all of the tumors showed a 31% increase in signal intensities at a 4.0-mg/kg dose, but all primary and metastatic tumors exhibited a 24–113% increase in signal intensities at a dose of 5.4 mg/kg.

A combined phase Ib/II clinical trial was reported by Carde et al. to investigate the effect of 10 daily intravenous doses of MGd with concomitant WBRT (23). The MTD, DLT, pharmacokinetics, and biolocalization were determined in patients with metastases in conjunction with a 30-Gy WBRT in 10 daily fractions (23). In the phase Ib part of the trial, MGd dose was escalated from 0.3 mg/kg to 8.4 mg/kg in 39 patients. In the phase II part of the trial, 22 patients received 5 - 6.3 mg/kg. The drug-related toxicity was assessed *via* complete blood counts and blood chemistry, urinalysis, history, and physical examination. Patients from both groups demonstrated satisfied tolerance to the 10 once-daily treatments. The MTD was found to be 6.3 mg/kg with reversible liver toxicity. The frequency of liver toxicity did not increase with dose, but the magnitude of changes in liver functions increased with increasing dose. Overall (phases Ib and II), 12 patients (19.6%) experienced liver toxicity of any grade. and 10 patients (16%) experienced grade 3 or 4 toxicity. The most common grade 3 and grade 4 adverse events were noted in 2 patients: hepatotoxicity, hypertension, brain edema, and vomiting. The most frequent adverse events observed with repeated administration of MGd were dose-dependent, transient, greenish skin (56%) and urine (43%) discoloration, as well as scleral discoloration (18%). The other adverse events noted in at least 10% of the patients were nausea (28%), vomiting (18%), asthenia (15%), rash (13%), headache (10%), abdominal pain (10%), and pruritus (10%). On the basis of these results, a regimen of 10 once-daily doses of MGd at 5 mg/kg in conjunction with a 30-Gy WBRT in 10 daily fractions was used in phase III trials to explore the effect of MGd in conjunction with WBRT on neurocognitive function and progression in patients with brain metastases from solid tumors (12, 13, 24). No further drug-related toxicity was reported in these phase III trials.

## NIH Support

AI 28845, CA 68682

## References

1. Kessel D. Porphyrin localization: a new modality for detection and therapy of tumors. Biochem Pharmacol. 1984;33(9):1389–93. PubMed PMID: 6233983.
2. Ogan M.D., Revel D., Brasch R.C. Metalloporphyrin contrast enhancement of tumors in magnetic resonance imaging. A study of human carcinoma, lymphoma, and fibrosarcoma in mice. Invest Radiol. 1987;22(10):822–8. PubMed PMID: 3429177.

3. Lyon R.C., Faustino P.J., Cohen J.S., Katz A., Mornex F., Colcher D., Baglin C., Koenig S.H., Hambright P. Tissue distribution and stability of metalloporphyrin MRI contrast agents. Magn Reson Med. 1987;4(1):24–33. PubMed PMID: 3821476.
4. Chen C.W., Cohen J.S., Myers C.E., Sohn M. Paramagnetic metalloporphyrins as potential contrast agents in NMR imaging. FEBS Lett. 1984;168(1):70–4. PubMed PMID: 6705923.
5. Lauffer R.B., Brady T.J., Brown R.D. 3rd, Baglin C., Koenig S.H. 1/T1 NMRD profiles of solutions of Mn2+ and Gd3+ protein-chelate conjugates. Magn Reson Med. 1986;3(4):541–8. PubMed PMID: 3747815.
6. Sessler J.L., Murai T., Hemmi G. A water-stable gadolinium (III) complex derived from a new pentadentate "expanded porphyrin" ligand. Inorg. Chem. 1989;28:3390–3393.
7. Sessler J.L., Mody T.D., Hemmi G.W., Lynch V. Synthesis and structural characterization of lanthanide(III) texaphyrins. Inorg. Chem. 1993;32:3175–87.
8. Sessler, J.L., G. Hemmi, T.D. Mody, T. Murai, A. Burrell, and S.w. Young, Texaphyrins: synthesis and applications. Acc. Chem. Res., 1994. 27(43-50): p. 43.
9. Richards G.M., Mehta M.P. Motexafin gadolinium in the treatment of brain metastases. Expert Opin Pharmacother. 2007;8(3):351–9. PubMed PMID: 17266469.
10. Young S.W., Sidhu M.K., Qing F., Muller H.H., Neuder M., Zanassi G., Mody T.D., Hemmi G., Dow W., Mutch J.D.et al. Preclinical evaluation of gadolinium (III) texaphyrin complex. A new paramagnetic contrast agent for magnetic resonance imaging. Invest Radiol. 1994;29(3):330–8. PubMed PMID: 8175308.
11. Magda D., Miller R.A. Motexafin gadolinium: a novel redox active drug for cancer therapy. Semin Cancer Biol. 2006;16(6):466–76. PubMed PMID: 17112739.
12. Mehta M.P., Rodrigus P., Terhaard C.H., Rao A., Suh J., Roa W., Souhami L., Bezjak A., Leibenhaut M., Komaki R., Schultz C., Timmerman R., Curran W., Smith J., Phan S.C., Miller R.A., Renschler M.F. Survival and neurologic outcomes in a randomized trial of motexafin gadolinium and whole-brain radiation therapy in brain metastases. J Clin Oncol. 2003;21(13):2529–36. PubMed PMID: 12829672.
13. Meyers C.A., Smith J.A., Bezjak A., Mehta M.P., Liebmann J., Illidge T., Kunkler I., Caudrelier J.M., Eisenberg P.D., Meerwaldt J., Siemers R., Carrie C., Gaspar L.E., Curran W., Phan S.C., Miller R.A., Renschler M.F. Neurocognitive function and progression in patients with brain metastases treated with whole-brain radiation and motexafin gadolinium: results of a randomized phase III trial. J Clin Oncol. 2004;22(1):157–65. PubMed PMID: 14701778.
14. Mehta M.P., Shapiro W.R., Glantz M.J., Patchell R.A., Weitzner M.A., Meyers C.A., Schultz C.J., Roa W.H., Leibenhaut M., Ford J., Curran W., Phan S., Smith J.A., Miller R.A., Renschler M.F. Lead-in phase to randomized trial of motexafin gadolinium and whole-brain radiation for patients with brain metastases: centralized assessment of magnetic resonance imaging, neurocognitive, and neurologic end points. J Clin Oncol. 2002;20(16):3445–53. PubMed PMID: 12177105.
15. Khuntia D., Mehta M. Motexafin gadolinium: a clinical review of a novel radioenhancer for brain tumors. Expert Rev Anticancer Ther. 2004;4(6):981–9. PubMed PMID: 15606327.
16. Motexafin gadolinium: gadolinium (III) texaphyrin, gadolinium texaphyrin, Gd-Tex, GdT2B2, PCI 0120. Drugs R D. 2004;5(1):52–7. PubMed PMID: 14725495.
17. Geraldes C.F., Sherry A.D., Vallet P., Maton F., Muller R.N., Mody T.D., Hemmi G., Sessler J.L. Nuclear magnetic relaxation dispersion studies of water-soluble gadolinium(III)-texaphyrin complexes. J Magn Reson Imaging. 1995;5(6):725–9. PubMed PMID: 8748493.
18. De Stasio G., Rajesh D., Ford J.M., Daniels M.J., Erhardt R.J., Frazer B.H., Tyliszczak T., Gilles M.K., Conhaim R.L., Howard S.P., Fowler J.F., Esteve F., Mehta M.P. Motexafin-gadolinium taken up in vitro by at least 90% of glioblastoma cell nuclei. Clin Cancer Res. 2006;12(1):206–13. PubMed PMID: 16397044.
19. Young S.W., Qing F., Harriman A., Sessler J.L., Dow W.C., Mody T.D., Hemmi G.W., Hao Y., Miller R.A. Gadolinium(III) texaphyrin: a tumor selective radiation sensitizer that is detectable by MRI. Proc Natl Acad Sci U S A. 1996;93(13):6610–5. PubMed PMID: 8692865.
20. Sessler, J.L., T.D. Mody, V. Lynch, S.W. Young, and R.A. Miller, Gadolinium(III) texaphyrin: a novel MRI contrast agent. J. Am. Chem. Soc., 1993. 115(10368-9): p. 10368.

21. Rosenthal D.I., Nurenberg P., Becerra C.R., Frenkel E.P., Carbone D.P., Lum B.L., Miller R., Engel J., Young S., Miles D., Renschler M.F. A phase I single-dose trial of gadolinium texaphyrin (Gd-Tex), a tumor selective radiation sensitizer detectable by magnetic resonance imaging. Clin Cancer Res. 1999;5(4):739–45. PubMed PMID: 10213207.
22. Rosenthal D.I., Becerra C.R., Toto R.D., Carbone D.P., Frenkel E.P. Reversible renal toxicity resulting from high single doses of the new radiosensitizer gadolinium texaphyrin. Am J Clin Oncol. 2000;23(6):593–8. PubMed PMID: 11202804.
23. Carde P., Timmerman R., Mehta M.P., Koprowski C.D., Ford J., Tishler R.B., Miles D., Miller R.A., Renschler M.F. Multicenter phase Ib/II trial of the radiation enhancer motexafin gadolinium in patients with brain metastases. J Clin Oncol. 2001;19(7):2074–83. PubMed PMID: 11283141.
24. Mehta M.P., Suh J.H. Novel radiosensitizers for tumors of the central nervous system. Curr Opin Investig Drugs. 2004;5(12):1284–91. PubMed PMID: 15648950.